

**Electronic Supplementary Information**

**Robust, non-fouling liters-per-day flow synthesis  
of ultra-small catalytically active metal  
nanoparticles in a single-channel reactor**

*Wai Kuan Wong, Swee Kun Yap, Yi Chen Lim and Saif A. Khan\**

Department of Chemical and Biomolecular Engineering, 4 Engineering Drive 4, National  
University of Singapore, Singapore 117585, Singapore

*Frédéric Pelletier and Elena Cristina Corbos*

Johnson Matthey Technology Centre, Blounts Court, Sonning Common, Reading RG4 9NH,  
United Kingdom

## COMPARISON WITH SINGLE-PHASE AND BIPHASIC REACTORS

The effectiveness of the abovementioned triphasic reactor in circumventing fouling and capturing evolved gaseous by-product was evaluated by comparing with the synthesis of PdNPs in a single-phase reactor and a biphasic reactor. For the single phase reactor, the palladium precursor solution and sodium borohydride are dispensed at the Y-junction as demonstrated in Figure S1 (a), where the Pd (II) is rapidly reduced to form PdNPs. The reaction occurs at the Y-junction once both solutions come into contact, and is accompanied with the rapid liberation of hydrogen gas. This creates significant pressure which resists the flow of reagents, eventually leading to back-flow of the combined reaction mixture into the reagent tubes. Subsequently, severe fouling occurs on the wall of reagent tube and inside the Y-junction, and a pulsing flow in the reactor tube with a large amount of gas bubbles held up on the reactor wall is observed, as shown in Figure S1 (b) and (c). The abovementioned flow characteristics significantly disrupt the stability of the reactor, and the inconsistent flow regime and flow rate during an extended period of reactor operation adversely affects the quality of the synthesized nanoparticles.

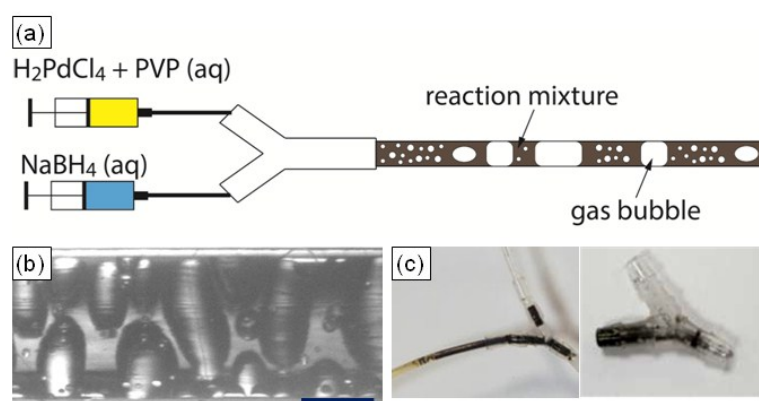


**Figure S1.** (a) Schematic of single-phase flow reactor for ultra-small nanoparticles synthesis; nucleation and growth of nanoparticles is initiated upon the contact of precursor solution and strong reducing agent at the Y-junction. (b) High-speed stereomicroscopic images of flow after Y-junction, highlighting a significant amount of gas bubbles accumulated within the reactor channel. The scale bar represents 0.5 mm. (c) Photograph of the reagent tubes and Y-junction, illustrating the back-flow of reaction mixture into the reagent tubes and deposition of nanoparticles at the Y-junction.

In the biphasic reactor, a regular biphasic flow is generated by combining silicone oil and palladium precursor solution to the first T-junction as displayed in Figure S2(a), which surrounds the aqueous precursor slugs with silicone oil as the continuous phase. At the second T-junction, sodium borohydride is injected into the aqueous slugs to initiate the formation of PdNPs, and results in the evolution of molecular hydrogen. Once the concentration of hydrogen exceeds the aqueous solubility threshold, hydrogen bubbles nucleate and grow uncontrollably in the reactor channel, forming an irregular, triphasic flow as shown in Figure S2 (b) and (c). With this reactor design, fouling issues are mitigated through isolation of the reaction mixture from the reactor wall through the usage of silicone oil. However, the uncontrolled liberation of hydrogen gas bubbles disrupts intra-slug mixing in the reactor channel, causing uneven distribution of reagents in the reactor slugs, thereby leading to undesirable and inconsistent nanoparticle characteristics, which include broad particle size distribution and low catalytic activity.

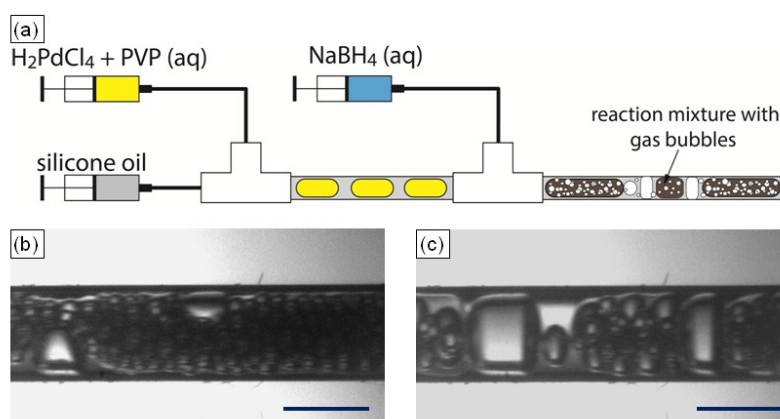


**Figure S2.** (a) Schematic of biphasic droplet flow reactor for ultra-small nanoparticles synthesis; a droplet flow with silicone oil surrounding the aqueous precursor slug is first formed in T-junction, followed by injection of introduction of aqueous sodium borohydride via the second T-junction to initiate the nucleation and growth of nanoparticles. (b) High-speed stereomicroscopic image of biphasic flow upon the introduction of sodium borohydride, demonstrating uncontrollable nucleation of large amount of small gas bubbles in the reactor channel. (c) High-speed stereomicroscopic image

of biphasic flow at the downstream of reactor channel, highlighting inconsistency in the flow with uncontrolled gas segments. All scale bars represent 1 mm.

In contrast to the single-phase reactor and biphasic reactor setups, the fouling and uncontrollable liberation of gaseous by-product can be mitigated via the triphasic flow design detailed in the main text, which maintains a consistent flow regime throughout continuous reactor operation. This enables the synthesis of nanoparticles with desirable attributes, such as high catalytic activity, ultra-small nanoparticle size (<5nm) and monodisperse particle size distribution.

## **DETERMINATION OF MIXING TIME IN BATCH AND TRIPHASIC MILLIFLUIDIC REACTOR FOR PDNPS SYNTHESIS**

### **Mixing time in small scale batch reactor**

To compare the quality of flow-synthesized PdNPs, 10 ml of 4mM PdNPs aqueous solution is produced in a small scale batch reactor ( $d_{\text{flask}} = 3.5$  cm) with a small magnetic stirrer ( $d_{\text{imp}} = 1.2$  cm). Based on the simple approach provided by Hartman et al.,<sup>1</sup> the mixing time in our small scale batch reactor for PdNPs synthesis is ~11s. First, the mixing regime of the batch reactor can be identified with Reynolds number of a vessel impeller (Equation 1). Impeller speed  $N$  is 20 rps, converted from stirring rate of 1200 rpm. Since this is a dilute aqueous solution, fluid density,  $\rho$  and fluid viscosity,  $\mu$  are estimated to be 1000 kg/m<sup>3</sup> and 0.001 kgm<sup>-1</sup>s<sup>-1</sup> respectively. The mixing regime in our batch reactor falls under transitional regime as the Reynolds number is 2880. After that, the mixing time of the batch reactor can be estimated from Equation 2.

$$Re = \frac{\rho N d_{\text{imp}}}{\mu} = 2880 \quad \text{----- (1)}$$

$$t_{\text{mixing}} = \frac{183^2}{N Re N_p^3} \left( \frac{d_{\text{flask}}}{d_{\text{imp}}} \right)^2 = 11s \quad \text{----- (2)}$$

### Mixing time in aqueous slugs within the triphasic reactor

In our triphasic millifluidic reactor, the synthesis of PdNPs takes place in the aqueous slugs which are miniaturized well-stirred batch reactors. There are two internal recirculation zones in each slug resulting from the relative motion between the boundaries of the droplets and the wall of the reactor.<sup>2,3</sup>

The mixing time in each slug can be approximated by equating the characteristic diffusion time and the time taken for convective transport. The diffusion time ( $t_D$ ) can be estimated based on Equation 3. The striation thickness is the characteristic length scale for diffusion; in this case, it is tube radius scaled by a factor  $2^{-n}$  in a slug with chaotic advection, where  $n$  is the number of convective cycles in a moving slug.<sup>4</sup> The diffusivity of Pd precursor and sodium borohydride is assumed to be  $\sim 10^{-9} \text{ m}^2\text{s}^{-1}$ .

$$t_D = \frac{\text{striation thickness}^2}{\text{diffusivity}} = \frac{\left(\frac{0.5}{1000} \times 2^{-n}\right)^2}{10^{-9}} \text{-----(3)}$$

At the other end, the time taken for a single convective cycle ( $t_c$ ) can be determined by dividing the perimeter of the slug by the flow speed. The diameter of PTFE tube is 1 mm and the flow speed for the triphasic flow is  $\sim 300 \text{ mm/s}$ . Based on the analysis of high-speed stereomicroscopic images, the average length of slug is  $\sim 3.3 \text{ mm}$ . Next, the time taken to achieve the striation thickness through convective transport  $t_{conv}$  can be estimated through Equation 5, where  $n$  is the number of convective cycles in a moving slug. Equating equations (3) and (5), and solving for  $n$  allows us to estimate the mixing time in each slug to be  $\sim 150 \text{ ms}$ .

$$t_c = \frac{0.5 + 3.3 + 0.5 + 3.3}{300} = 0.025 \text{ s} \text{-----(4)}$$

$$t_{conv} = 0.025 n \text{-----(5)}$$

**INVESTIGATION OF PDNPS CATALYTIC ACTIVITY USING TRIPHASIC FLOW REACTOR FOR HYDROGENATION OF 1-HEXENE**

**Comparison between batch and flow synthesized PdNPs**

PdNPs	Residence time (s)	Conversion (%)	Activity ( $\text{mol}_{\text{hexane}}\text{mol}_{\text{PdNPs}}^{-1}\text{s}^{-1}$ )
Batch synthesized	22	48	6.2
Flow synthesized	22	77	11.9

**Table S1.** Comparison between the catalytic activities of flow and batch synthesized PdNPs, which are assessed using a triphasic flow reactor for hydrogenation of 1-hexene at room temperature and pressure using 1 mM of PdNP solution.

**Catalytic activity of PdNPs for hourly samples from the 6-hour run**

PdNPs	Residence time (s)	Run 1		Run 2	
		Conversion (%)	Activity ( $\text{mol}_{\text{hexane}}\text{mol}_{\text{PdNPs}}^{-1}\text{s}^{-1}$ )	Conversion (%)	Activity ( $\text{mol}_{\text{hexane}}\text{mol}_{\text{PdNPs}}^{-1}\text{s}^{-1}$ )
0 <sup>th</sup>	20	81	12.4	73	11.4
1 <sup>st</sup>	20	61	10.0	78	12.9
2 <sup>nd</sup>	20	78	12.4	72	11.9
3 <sup>rd</sup>	20	86	13.6	59	9.7
4 <sup>th</sup>	20	85	13.4	75	11.9
5 <sup>th</sup>	20	79	12.5	78	12.5
6 <sup>th</sup>	20	74	11.6	80	12.5

**Table S2.** Catalytic activities of PdNPs, for hourly samples from two separate 6-hour nanoparticle production runs

## References

1. R. L. Hartman, J. P. McMullen and K. F. Jensen, *Angew Chem Int Ed Engl*, 2011, **50**, 7502-7519.
2. H. Song, D. L. Chen and R. F. Ismagilov, *Angew Chem Int Ed Engl*, 2006, **45**, 7336-7356.
3. H. Song, J. D. Tice and R. F. Ismagilov, *Angewandte Chemie International Edition*, 2003, **42**, 768-772.
4. M. R. Bringer, C. J. Gerdtts, H. Song, J. D. Tice and R. F. Ismagilov, *Philosophical Transactions of the Royal Society of London. Series A: Mathematical, Physical and Engineering Sciences*, 2004, **362**, 1087-1104.